2.1 NUMERICAL SIMULATION OF PULSATING BORA WIND GUSTS

Danijel Belušić[1]*, Mark Žagar[2] and Branko Grisogono[1]
[1]University of Zagreb, Zagreb, Croatia
[2]Environmental Agency of Slovenia, Ljubljana, Slovenia

1. INTRODUCTION

Bora wind is a relatively cold, predominantly northeasterly downslope windstorm blowing down the western side of the Dinaric Alps and plunging on the Adriatic Sea. Bora winds may reach mean wind speeds of over 20 m s^{-1}. Many previous studies have examined the multi-scale bora nature using measurements, numerical simulations or theoretical concepts. Lately, a strong emphasis has been given to the interaction between the bora and the Adriatic using state-of-the-art coupled numerical models (e.g. Pullen et al., 2007).

However, the bora main feature is its gustiness. The maximum bora gusts are almost twice the hourly mean wind speeds, which brings the bora wind to hurricane strengths when gusts surpass 50 or even 60 m s^{-1}. It has been shown that the temporal variability of bora gusts stems from the superposition of two components: 3–8 min quasi-periodic oscillations (i.e. pulsations) and high-frequency local turbulence (e.g. Belušić et al., 2006). The pulsating component has also been reported in other similar winds, e.g. the Boulder downslope windstorm (e.g. Neiman et al., 1988). Previously proposed generating mechanisms of the pulsations include Kelvin-Helmholtz instability (KHI), vortex tilting in the wave-breaking region and propagating lee waves (e.g. Belušić et al., 2007). Recently, the possibility of disappearance of the pulsations within a bora episode has been reported (Belušić et al., 2004). The peculiarity is that even when the pulsations are absent, the mean bora wind speed remains intact.

This study employs a high-resolution numerical simulation for examination of the bora wind properties in situations both with and without pulsations. The period of interest is 8 – 9 December 2001.

2. SYNOPTIC SITUATION

A cut-off low was present above Greece with associated northeasterly winds at 300 hPa. The maximum wind speed above the northern Adriatic region increased to over 35 m s^{-1} on 9 December 2001 due to shifting of the upper-level ridge towards the east (Fig. 1).

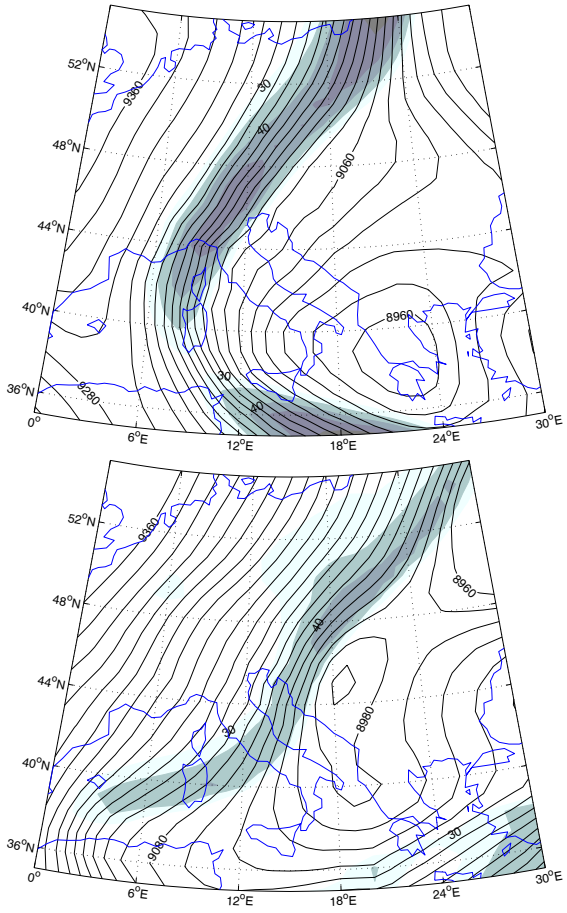

Figure 1. 300 hPa geopotential (contour interval 20 gpm) and wind speed (shaded, interval 5 m s^{-1}) at 06 UTC 8 Dec (up) and 06 UTC 9 Dec (down) 2001.

3. NUMERICAL SIMULATION

The atmospheric component of the non-hydrostatic, fully compressible mesoscale model COAMPS™ (Hodur, 1997) has been used. Four nested domains have been used, with grid spacing of 9, 3, 1 and 0.33 km and 51 x 51, 61 x 61, 91 x 91 and 91 x 91 grid points, respectively (Fig. 2). There were 81 vertical levels reaching the height of 24 km, with higher vertical resolution near the surface and lower near the model top. For details of the model setup see Belušić et al. (2007). The model output is given every 30 s at Senj and 50 s for 3D fields. The start of the simulation is at 00 UTC 8 December 2001. The initial and boundary conditions are obtained from the ECMWF operational analyses.

* *Corresponding author address:* Danijel Belušić, University of Zagreb, Faculty of Science, Dept. of Geophysics, Zagreb, Croatia, email: dbelusic@irb.hr.

All model data presented here are taken from the 1-km domain, except for the analysis in Section 7.

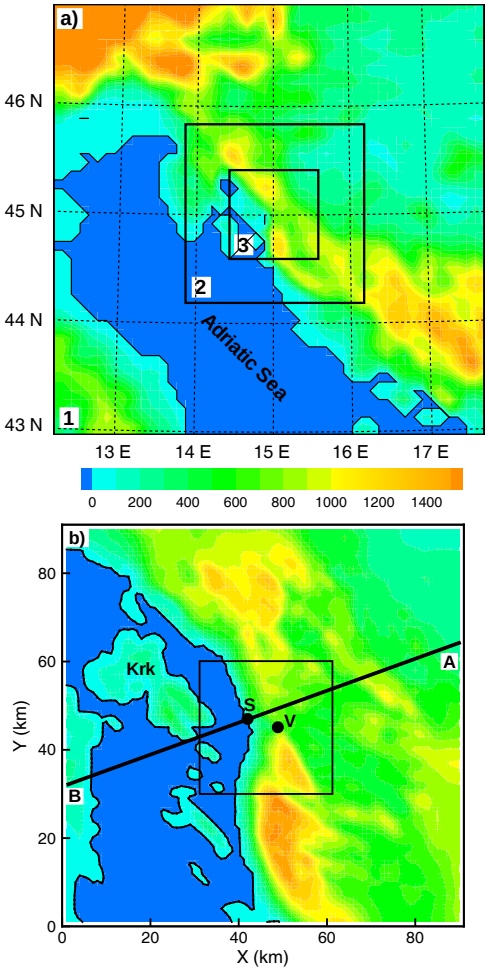

Figure 2. Model domains; terrain contour interval 100 m. a) Domain 1 (9 km) with indicated domains 2 (3 km) and 3 (1 km). b) Domain 3 with indicated domain 4 (333 m). The line AB denotes the vertical cross-sections shown in Fig. 6. S and V denote Senj and Vratnik Pass.

4. DATA

The measurements were undertaken in Senj (44.99°N, 14.90°E, 2 m MSL) at 13 m AGL with a cup anemometer at 1 Hz sampling frequency (for details see Belušić et al., 2004). The coordinate system has been rotated so that the *u* component is in the along-wind direction. All subsequent analysis is performed on this rotated *u* component.

5. MODEL PERFORMANCE AT SENJ

Figure 3 depicts the time series comparison between the simulated and measured *u* at Senj. In terms of hourly averages, the model performed quite well except between hours 17 and 23, where the model did not capture the cessation of the bora. The fine-scale model variability seems to underestimate the recorded one.

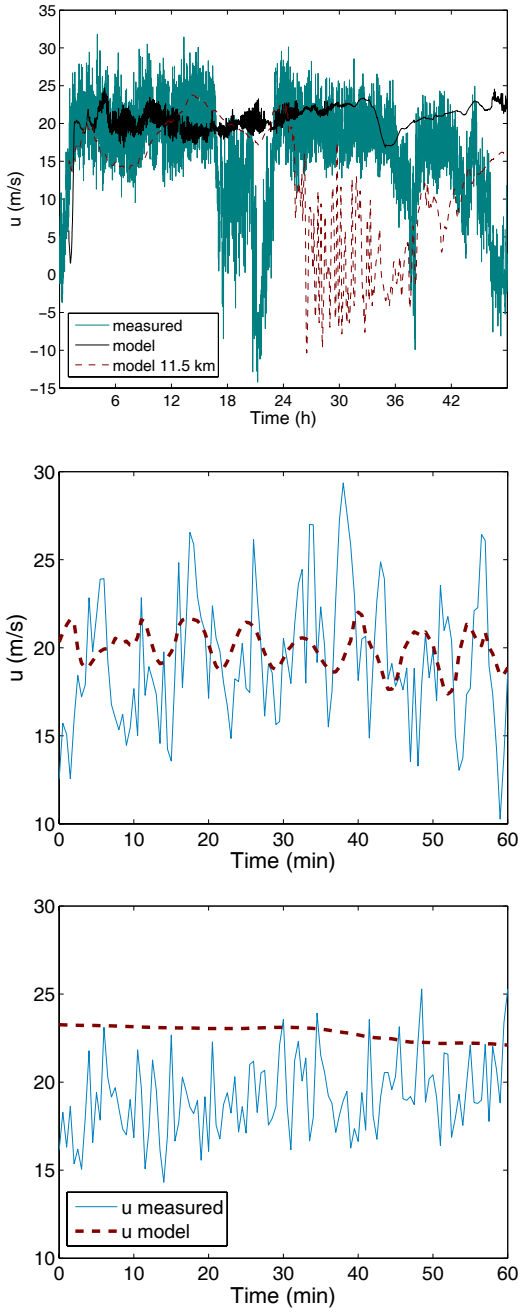

Figure 3. Measured vs. modeled time series of 30-s *u* at Senj. Upper panel: Near-surface *u* with *u* at 11.5 km AGL. Time is in hours after 00 UTC 8 Dec 2001. Zoomed 1-h periods with (middle panel; 340th–400th min of the simulation) and without (lower panel; 1960th–2020th min of the simulation) pulsations near the surface.

The fine-scale variability in the model is seen in the first part of the episode. Exactly this part of the episode is characterized by pulsations in the

measured data, which can be seen in the 1-h zoomed series in Fig. 3. It is seen that the model reproduced the pulsations well. The finer-scale non-periodic variability that is superimposed on the pulsations in the measurements was not reproduced by the model. This is expected from this kind of models and is also of no importance for our study, which emphasizes the pulsations.

Figure 4 further corroborates the success of the model in the range of frequencies of pulsations (i.e. periods around 7 min).

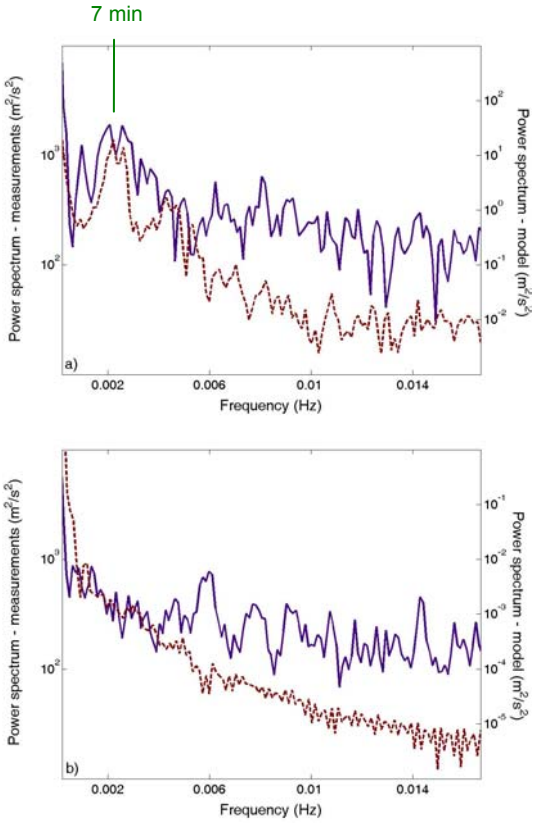

Figure 4. Power spectral density of measured (solid violet) and modelled (dashed red) near-surface *u* at Senj. Upper panel: Presence of pulsations in the first part of the episode (hours 3–15.5). Lower panel: Pulsations are absent in the second part of the episode (hours 31–45.2; see Fig. 3).

6. FLOW STRUCTURE

Figure 5 depicts the horizontal view of situations with and without pulsations. There are the usual jets and wakes that extend over the sea when the pulsations are present. During the absence of pulsations there is only the jet from the Vratnik Pass with lower wind speeds away from the mountain than in the case with pulsations, while the flow reversal occurs between the land and the Island of Krk. This points to the occurrence of a mountain wave induced rotor during the situation without pulsations, as discussed in Belušić et al. (2007).

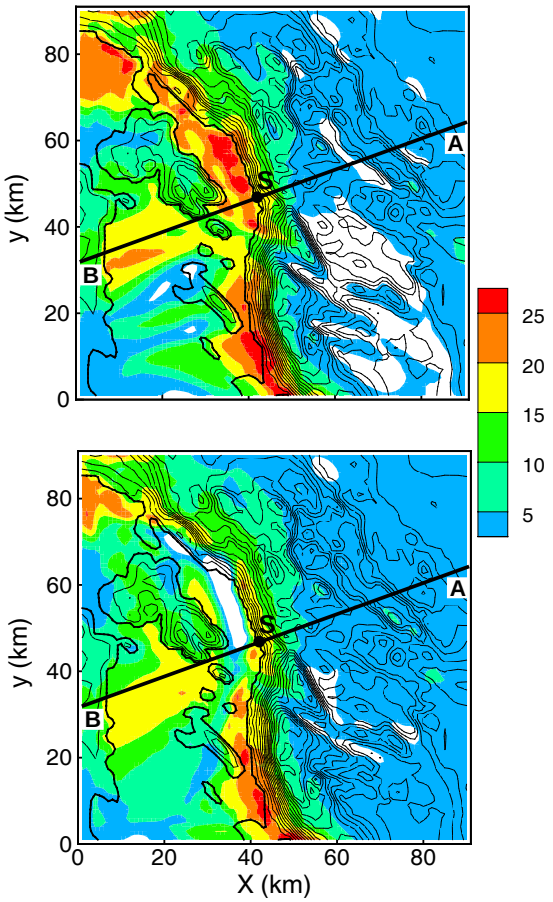

Figure 5. Horizontal cross-sections of *u* near the surface. Upper panel: Pulsations are present (10 LST 8 Dec). Lower panel: Pulsations are absent (13 LST 9 Dec). The line AB denotes the vertical cross-sections shown in Fig. 6. S denotes Senj.

Figure 6 shows the corresponding vertical cross-sections for the two situations. The low-level wave breaking is present in the situation with pulsations. Also, there is a strong low-level shooting flow beneath the wave-breaking region and the offshore boundary layer jump (Fig. 6, upper panel). Therefore, as seen in both horizontal and vertical, this situation resembles the usual setup of the strong bora (e.g. Belušić and Klaić, 2006). To the contrary, when the pulsations are absent the low level setup is characterized by large-amplitude trapped lee waves (Fig. 6, lower panel). Hence, there is no significant low-level wave breaking. This implies that the magnitude of the low-level negative shear between the bora jet and the usual stagnant, now absent, wave-breaking region is reduced and hence the Richardson number which is a measure of dynamical stability is increased.

It is interesting to note that in the case without pulsations the wave breaking occurs around the tropopause level instead. This is the

origin of the variability of *u* at 11.5 km seen in Fig. 3.

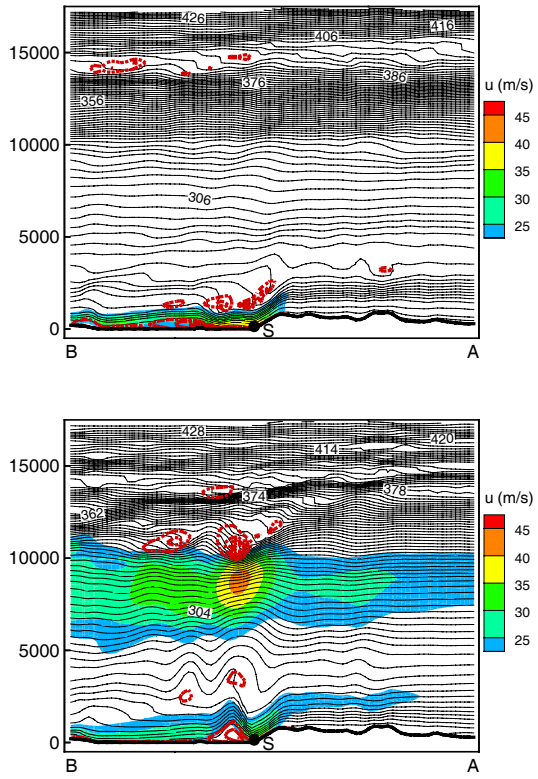

Figure 6. Vertical cross-sections corresponding to Fig. 5 along the line AB. Shown are potential temperature contours (2 K interval), wind speed along the cross-section (color) and TKE (red dashed, starts at 2 J kg^{-1} with 2 J kg^{-1} (upper panel) and 6 J kg^{-1} (lower panel) interval).

7. DETAILED STRUCTURE OF PULSATIONS

Figure 7 shows the horizontal view of a pulsation development, while Fig. 8 depicts its vertical structure. The four panels span an interval of 5 min, which is approximately the period of pulsations. In the horizontal, pulsations have almost elliptical shape. They propagate downstream and eventually fade away.

Vertical cross-sections (Fig. 8) show that the pulsation is generated when the shear strengthens. The creation of the pulsation relaxes the strong shear below the wave breaking and hence reduces the dynamic instability, i.e. the Richardson number increases (not shown). Afterwards, the shear strengthens again and the rhythmical process is repeated. This is in accordance with the KHI mechanism (see further discussion in Belušić et al., 2007).

8. CONCLUSIONS

A fine-scale numerical simulation of a bora event is presented with the goal to examine the properties of pulsating bora wind gusts. The chosen bora event is characterized by the presence of pulsations in the first part and their absence in the second part. This provides an opportunity to study the detailed changes in the flow structure that lead to the disappearance of pulsations, while high near-surface wind speeds remain. It is shown that when the pulsations are present the flow is as in the usual strong-bora setup. On the other hand, when the pulsations are absent the low-level wave breaking is replaced by large-amplitude lee waves that can sustain strong near-surface wind speeds close to the mountain. This is consistent with the results of Zängl and Hornsteiner (2007).

The generating mechanism of the pulsations appears to be KHI in this case.

ACKNOWLEDGMENTS

The work was supported by the Croatian Ministry of Science, Education and Sports (projects 119-1193086-1323 and 119-1193086-1311).

REFERENCES

Belušić, D., M. Pasarić, and M. Orlić, 2004: Quasi-periodic bora gusts related to the structure of the troposphere. *Q. J. R. Meteorol. Soc.*, **130**, 1103–1121.

Belušić, D., and Z. B. Klaić, 2006: Mesoscale dynamics, structure and predictability of a severe Adriatic bora case. *Meteorol. Z.*, **15**, 157–168.

Belušić, D., M. Pasarić, Z. Pasarić, M. Orlić, and B. Grisogono, 2006: A note on local and non-local properties of turbulence in the bora flow. *Meteorol. Z.*, **15**, 301–306.

Belušić, D., M. Žagar, and B. Grisogono, 2007: Numerical simulation of pulsations in the bora wind, *Q. J. R. Meteorol. Soc.,* in press.

Hodur, R. M., 1997: The Naval Research Laboratory's Coupled Ocean/Atmosphere Mesoscale Prediction System (COAMPS). *Mon. Weather Rev.*, **125**, 1414–1430.

Neiman, P. J., R. M. Hardesty, M. A. Shapiro, and R. E. Cupp, 1988: Doppler lidar observations of a downslope windstorm. *Mon. Weather Rev.*, **116,** 2265–2275.

Pullen, J., J. D. Doyle, T. Haack, C. Dorman, R. P. Signell, and C. M. Lee, 2007: Bora event variability and the role of air-sea feedback, *J. Geophys. Res.*, **112**, C03S18, doi: 10.1029/2006JC003726.

Zängl, G., and M. Hornsteiner, 2007: Can trapped gravity waves be relevant for severe foehn windstorms? A case study. *Meteorol. Z.*, **16**, 203–212.

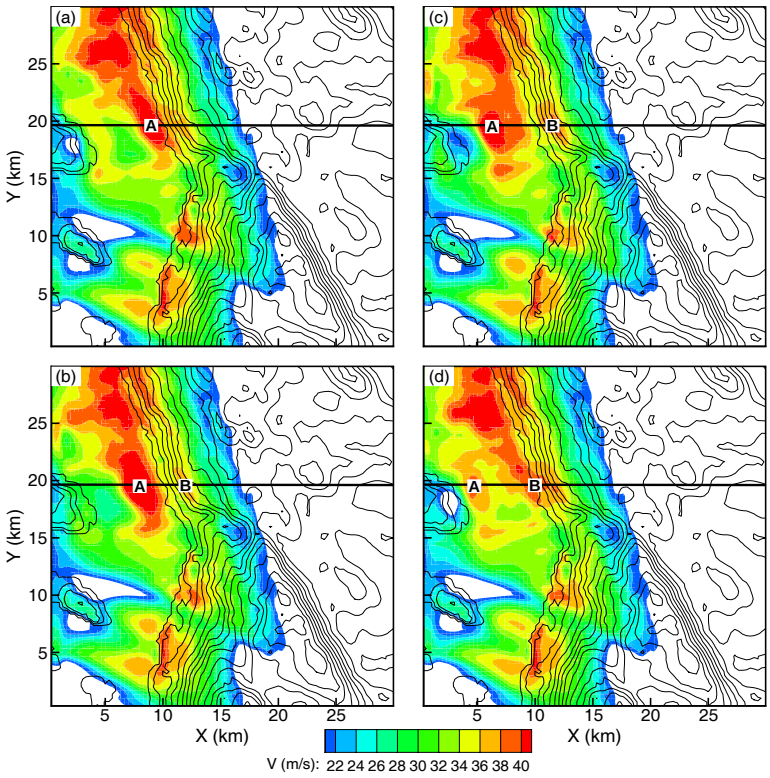

Figure 7. Horizontal view of a pulsation development over the period of 5 min (Δt between consecutive panels is 100 s). Shown is the wind speed magnitude. A and B denote individual pulsations.

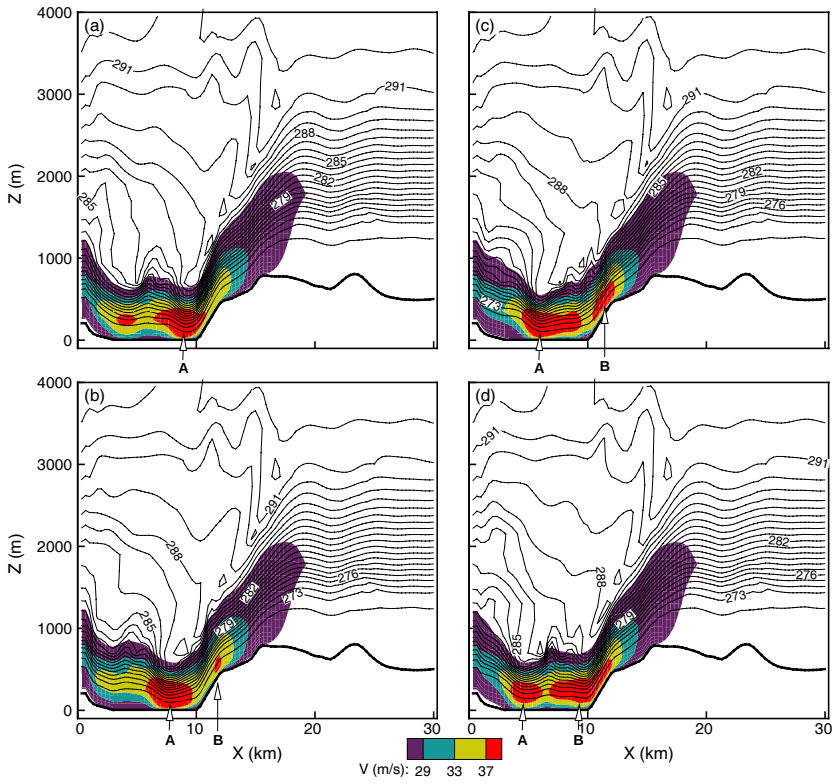

Figure 8. Vertical cross-sections corresponding to Fig. 7 along the horizontal line indicated in Fig. 7. Shown are the wind speed magnitude (color) and potential temperature contours (interval 1 K).